Published online April 1, 2004

1982–1992 *Nucleic Acids Research, 2004, Vol. 32, No. 6*
DOI: 10.1093/nar/gkh512

Fundamental structural units of the *Escherichia coli* nucleoid revealed by atomic force microscopy

Joongbaek Kim, Shige H. Yoshimura, Kohji Hizume, Ryosuke L. Ohniwa, Akira Ishihama[1] and Kunio Takeyasu*

Laboratory of Plasma Membrane and Nuclear Signaling, Graduate School of Biostudies, Kyoto University, Kitashirakawa Oiwake-cho, Sakyo-ku, Kyoto 606-8502, Japan and [1]Division of Molecular Biology, Nippon Institute for Biological Science, Shinmachi, Ome, Tokyo 198-0024, Japan

Received July 25, 2003; Revised December 25, 2003; Accepted March 9, 2004

ABSTRACT

A small container of several to a few hundred μm³ (i.e. bacterial cells and eukaryotic nuclei) contains extremely long genomic DNA (i.e. mm and m long, respectively) in a highly organized fashion. To understand how such genomic architecture could be achieved, *Escherichia coli* nucleoids were subjected to structural analyses under atomic force microscopy, and found to change their structure dynamically during cell growth, i.e. the nucleoid structure in the stationary phase was more tightly compacted than in the log phase. However, in both log and stationary phases, a fundamental fibrous structure with a diameter of ~80 nm was found. In addition to this '80 nm fiber', a thinner '40 nm fiber' and a higher order 'loop' structure were identified in the log phase nucleoid. In the later growth phases, the nucleoid turned into a 'coral reef structure' that also possessed the 80 nm fiber units, and, finally, into a 'tightly compacted nucleoid' that was stable in a mild lysis buffer. Mutant analysis demonstrated that these tight compactions of the nucleoid required a protein, Dps. From these results and previously available information, we propose a structural model of the *E.coli* nucleoid.

INTRODUCTION

The genome consists of a few million (bacteria) to a billion (eukaryotes) base pairs of DNA. This long genomic DNA is housed in a small container with a volume of several (bacterial cell) to a few hundred μm³ (eukaryotic nucleus) in a highly compacted but well-organized fashion.

In the case of eukaryotes, the genomic DNA is assembled into higher order structures under a balance of the physical properties of the double-stranded DNA and the mechanical effects of DNA–protein interactions (1,2). The major species of proteins associated with the genome are histones. In eukaryotes, ~150 bp long DNA wraps (about 1.75 turns) around a histone octamer (two of each of histone H2A, H2B, H3 and H4), and makes up a nucleosome, a basic unit of chromatin fibers (1,3–9). Such nucleosomes have been identified as a 'beads-on-a-string' structure by atomic force microscopy (AFM) (10–13) as well as by electron microscopy (14–17). However, higher order structures beyond this beads-on-a-string structure have not been successful targets of investigations. In the models currently believed, the basic chromatin fiber is thought to fold into 30 nm and/or thicker solenoid fibers, the formation of which is critical for the regulation of gene duplication and expression (18).

The formation of the nucleosome structure has been recognized as one of the basic differences between prokaryotes and eukaryotes. However, bacteria contain histone-like proteins, such as HU and IHF, which exist in the nucleoid, a bacterial form of the genome architecture (19–21). The HU proteins, like core histones in eukaryotes, form homo- or hetero-dimers and hetero-octamers (22–24) and are considered to play critical roles in the construction of nucleoids via the formation of a nucleosome-like structure (20,25). Because of the similarity in molecular properties between the eukaryotic histones and the prokaryotic histone-like proteins, the basic molecular mechanism of genome packing may be common in prokaryotes and eukaryotes. Thus, the bacterial nucleoid, which is smaller than the eukaryotic chromosome, can be a model system to understand the fundamental genome folding mechanism.

In this study, a nano-structural analysis utilizing AFM was applied to elucidate the higher order structure of the *E.coli* nucleoid. Since AFM allows molecular imaging at the nano-scale without sample fixation or staining, it successfully revealed the existence of a basic structural unit as seen in the eukaryotic chromosome. The mode of packaging of the nucleoids was found to change during cell growth.

MATERIALS AND METHODS

Bacterial strains and growth conditions

A well-isolated colony of the *E.coli* strains (K-12 W3110 and XL-1 blue) or a Dps-deficient mutant strain (Δ*dps*) of W3110 (26) on LB agar plate was transferred into 2 ml of LB medium and cultured at 37°C with constant shaking (220 r.p.m.) for 24 h. A 2 μl aliquot of the saturated culture was inoculated into 2 ml of fresh LB and cultured at 37°C with constant shaking

*To whom correspondence should be addressed. Tel/Fax: +81 75 753 6852; Email: takeyasu@lif.kyoto-u.ac.jp

(220 r.p.m.) to a certain cell density. The cell density was determined by the absorbance at a wavelength of 600 nm.

Cell lysis

The cells in different growing phases were collected by centrifugation (12 000 *g* at 0°C for 3 min), washed with 1× phosphate-buffered saline (PBS) and resuspended in 1× PBS. A 5 µl aliquot of the cell suspension was deposited onto a round coverglass 18 mm in diameter. The extra liquid on the coverglass was blown off by nitrogen gas and the coverglass was then dipped in 2 ml of a buffer containing 100 mM Tris–HCl pH 8.2, 0.1 M NaCl and 1 mM NaN_3. After 5 min, lysozyme was added to a final concentration of 25 µg/ml. After 1 min incubation, a detergent solution containing Brij 58 (polyoxyethylene hexadecylether) and sodium deoxycholate was added to a final concentration of 0.25 and 0.1 mg/ml, respectively. After 10 min, the coverglass was dried under nitrogen gas. The surface of coverglass was gently washed with distilled water and dried again.

Microscopy

The samples were visualized under an atomic force microscope (Seiko Instruments Inc.). The imaging was performed in a dynamic force mode (DFM) with a 150 µm scanner in air at room temperature. The cantilevers (Olympus) had a resonant frequency of ~300 kHz and a spring constant of 42 N/m. The scan was performed at 0.4 Hz, and images were captured in 512 × 512 pixel format. For the fluorescence microscopy, the sample was incubated in Hoechst 33258 solution (1 µg/ml in 1× PBS) for 1 min and then washed with PBS twice. The sample was observed under a fluorescence microscope (Axiovert 200, Zeiss) and the images were captured by a digital camera (AxioCam, Zeiss).

The analysis of the obtained AFM images was performed with an image analysis program accompanying the imaging module (Seiko Instruments). Two parameters were measured: the widths of isolated fibers and the peak-to-peak distances of connected fibers and beads. The width of an isolated fiber on an AFM image is affected by the tip size, whereas the peak-to-peak distance is not. Therefore, the real widths of the isolated fibers were obtained by measuring the widths at the half-maximum height (FWHM; full width at half-maximum). This procedure is able to subtract the size effect of the scanning tip as described previously (27).

Western blot analysis

Bacterial strain W3110 and the Dps-deficient mutant were grown in LB medium at 37°C and harvested after ~3 (log phase), ~7 (early stationary phase), 24, 48 and 72 h. The growth phase is determined by OD_{600}; log ($0.2 < OD_{600} < 1.0$), early stationary ($1.0 < OD600 < 2.0$). Cells were washed with PBS, freeze-thawed three times and re-suspended in SDS sample buffer (50 mM Tris–HCl pH 6.8, 2% SDS, 1% 2-mercaptoethanol, 10% glycerol, 0.025% bromophenol blue). An equal amount of the cell lysate was loaded onto each well and subjected to SDS–PAGE. The gels were analyzed either by Coomassie brilliant blue staining or by immunoblotting with polyclonal antibodies against Dps, HU and IHF.

Complementation of the Δ*dps* phenotype

The coding sequence for the Dps protein was amplified by PCR and subcloned into the pCA24N vector (28) by using StuI restriction sites. The green fluorescent protein (GFP) sequence in the pCA24N vector was deleted by SfiI restriction and the vector was renamed pHM44. The *dps* gene is now under the control of the pT5/*lac* promoter and the gene expression can be induced by isopropyl-β-D-thiogalactopyranoside (IPTG). The plasmid was then introduced into a *dps*-deficient strain of W3110. The cells at different growth phases were exposed to IPTG (5 mM) for varying periods of time and subjected to AFM analyses.

Search in the bacterial genome database

The orthologs of *E.coli* nucleoid proteins (CbpA, DnaA, CbpB, Dps, HU/IHF, Hfq, Fis, H-NS/StpA, IciA/LysR and Lrp/AsnC) in the other bacteria whose genome projects were completed were searched on SSDB (Sequence Similarity Database) (29). When orthologs or closely related homologs were not found in a certain species, a FASTA search of the genes and genomes was done on the KEGG database (Kyoto Encyclopedia of Genes and Genomes) (29) using the nucleoid proteins of interest as queries.

RESULTS

The nucleoid is fragile and its molecular structure changes drastically during its isolation and purification. Here we developed a procedure to mildly lyse bacterial cells on a coverslide so as to spread the nucleoid directly on the coverslide, followed by AFM imaging without any purification, fixation or staining steps. This cell lysis procedure was adapted from the previous study (30) with several modifications; the amounts of lysozyme and detergent were adjusted to optimize the lysis conditions, and the osmotic shock treatment was not employed in order to avoid any harsh effects on the nucleoid structure. Using the newly developed method, several novel and unique features of the bacterial nucleoid were identified.

Growth phase-dependent change in the overall structure of the nucleoid

Escherichia coli strain W3110 was grown in LB medium and harvested in the lag ($OD_{600} < 0.2$), log ($0.2 < OD_{600} < 1.0$), early stationary ($1.0 < OD600 < 2.0$) and late stationary ($OD_{600} > 2.0$) phases. The cells were attached onto a coverslide, lysed under mild conditions and stained with Hoechst 33258. Observation using a fluorescence microscope revealed different nucleoid structures in different growth phases (Fig. 1A–D). Thin fibers of DNA spreading out from the cell were observed in the log phase nucleoid (Fig. 1B). Towards the stationary phase, however, the DNA fibers became tightly compacted and hardly spread out (Fig. 1D). After this transition, the DNA fiber was never released from the nucleoid by the mild detergent treatment. These observations suggest that the DNA was compacted more tightly in the stationary phase than in the log phase. Upon re-start of the culture by inoculating the stationary phase cells into fresh medium, the nucleoid DNA re-entered a loosely packed state. The occurrence of these different architectural stages has been

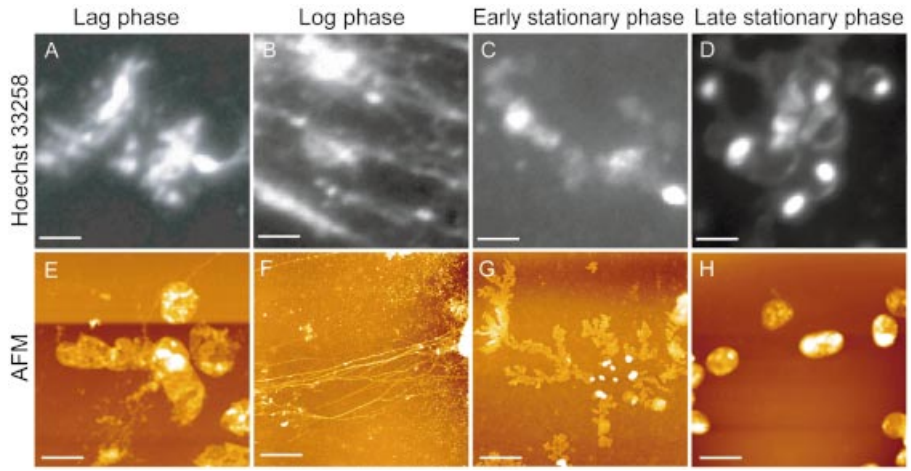

Figure 1. Overall structure of the nucleoid. *Escherichia coli* strain W3110 was grown in LB medium. The cells were attached to a coverglass and then mildly treated with lysozyme and detergent (see Materials and Methods). The cells were observed either by fluorescence microscopy after staining with Hoechst 33258 (A–D) or by AFM without staining (E–H). (**A** and **E**) Lag phase cells; (**B** and **F**) log phase cells; (**C** and **G**) early stationary phase cells; and (**D** and **H**) late stationary phase cells. Scale bars, 2 μm.

suggested by the previous study in which *E.coli* cells were lysed in agarose gel (31).

In parallel with the fluorescence microscopy, the nucleoid was subjected to AFM imaging without staining (Fig. 1E–H). In agreement with the observations by fluorescence microscopy, the nucleoid in the lag phase cells partially came out from the cell and spread on the coverslide (Fig. 1E). The nucleoid appears to consist of aggregations of small globular particles (~80 nm in diameter). In the log phase nucleoid, a number of thin fibers (~40 and ~80 nm in width) came out from the nucleoid (Fig. 1F), indicating that the nucleoid is easily loosened by the detergent treatment. In the early stationary phase, the nucleoid was also spread around, but no thin fiber was observed (Fig. 1G). This 'coral reef structure' was composed of a granular unit (~80 nm in diameter), suggesting that the 80 nm granular fiber is further tightly folded in the early stationary phase. The late stationary phase nucleoid remained tightly packed even after the lysis treatment (Fig. 1H). Thus, the overall packing of the nucleoid becomes tighter as the cells grow into the stationary phase. When the same procedure was applied to another bacterial strain, XL-1 blue, the same pattern of growth phase-dependent changes of the nucleoid structure was also observed (data not shown).

Fundamental structural unit of the nucleoid and its hierarchical structures

In the log phase nucleoid, which is most loosely packed during cell growth, thin fibers with two different widths (~40 and ~80 nm) were identified (Fig. 2A and C). These fibers correspond to the thin fibers identified by fluorescence microscopy, which are supposed to be composed of DNA and nucleoid-related proteins. The '80 nm fiber' apparently shows a solenoidal pitch of ~40 nm (Fig. 2A). Thus, the '40 nm fiber' could be a substructure of the 80 nm fiber. In partially lysed log phase cells, the 80 nm fiber formed a loop structure with ~150 nm inside diameter (Fig. 2B). These data suggest that the 40 nm fiber is a fundamental structural unit of the nucleoid, which can be folded up into the 80 nm fiber and further into a much higher order tight architecture in the stationary phase.

Fibers with granule-like structures were also observed in the lag, and early stationary phases. Since the nucleoids in these phases are less sensitive to the detergent, a released 40 nm fiber was not observed (Fig. 3A and B). Although a single well-separated 80 nm fiber was not obtained from these nucleoids, probably due to the tighter packing, the granular unit of 80 nm in diameter was clearly observed on the surface of these nucleoids (Fig. 2A and B). Judging from its stability against the lysis procedure and its occurrence throughout the growth phases, this '80 nm granular fiber' is one of the basic units of the nucleoid architecture. However, in the late stationary phase, this structure was drastically changed into a tightly compacted one that was resistant to the mild detergent treatment (Fig. 3C).

Dps plays a critical role in nucleoid compaction towards the stationary phase

The amount of each nucleoid-associated protein changes markedly during the growth phase transition from the log to the stationary phases (32). In the stationary phase, Dps (DNA-binding protein from starved cells) becomes the most abundant nucleoid component (180 000 molecules per nucleoid) (32). A genetic analysis has demonstrated that the expression of Dps is critical for survival under various kinds of stresses (26). Therefore, we examined the nucleoid architecture of the W3110 strain depleted of the Dps protein.

The wild-type strain and the mutant strain that had the *dps* gene deleted (Δ*dps*) (26) were cultured in LB medium and the intracellular protein compositions were analyzed by SDS–PAGE and immunoblotting. The Dps protein was hardly detected in the log phase, but was induced in the early stationary phase and remained present towards the late stationary phase in the wild-type cells (Fig. 4B, lanes 1–5). The induction of Dps (~22 kDa) in the stationary phase could be detected even with Coomassie brilliant blue staining.

On the other hand, no induction of Dps was observed in the *dps* mutant strain (lanes 6–10). The amounts of other nucleoid-related proteins (HU and IHF) were not affected by the depletion of Dps (Fig. 4C and D).

The *dps* mutant cells were subjected to the on-substrate lysis treatment and AFM observation. The detailed structure of the Dps-deficient log phase nucleoid was almost similar to that of the wild-type nucleoid; 40 and 80 nm fiber and loop structures were identified (Fig. 5A and B). However, in contrast to the wild-type cells, the Δ*dps* cells did not show a

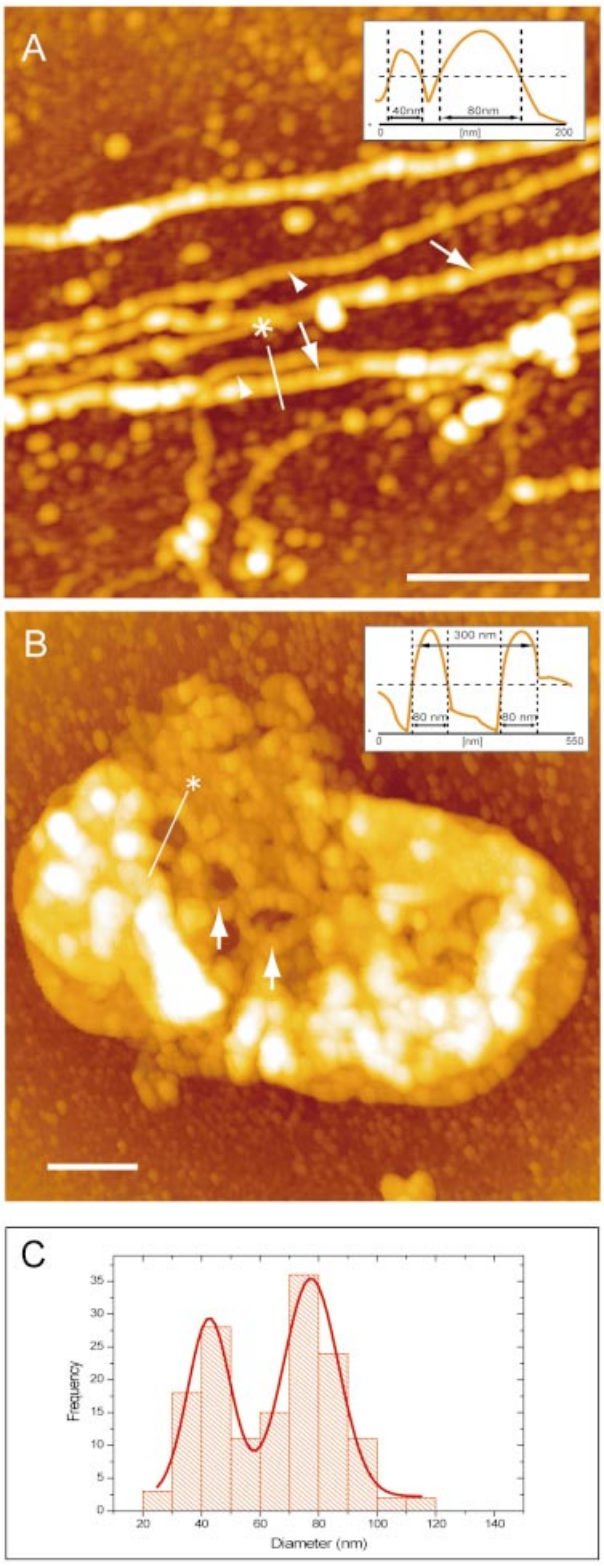

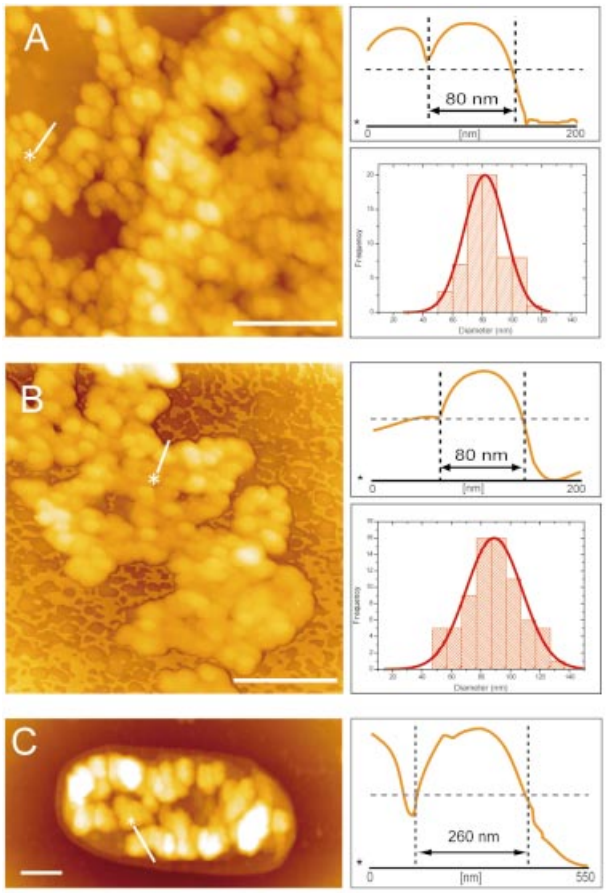

Figure 3. Tight packing of the nucleoid. Closer observations of the nucleoids in the lag (**A**) and early stationary (**B**) phase revealed the 80 nm granular structures. The solid lines represent the sites of section analysis that are depicted in the right upper panels. The horizontal dotted lines on section analysis images indicate the half-maximum height. The diameters of the granules were measured and are summarized in the right bottom panels (bin size, 10 nm). A peak curve obtained by Gaussian fitting was overlaid in each histogram. The peak-to-peak distance of adjacent beads in AFM images (B) was also measured and appeared to be ~80 nm (78.58 ± 20.13 nm, mean ± SD). A thick fiber in a tightly compacted nucleoid (**C**) was observed in the late stationary phase. The solid line in the AFM image represents the sites of section analysis that are depicted in the right panel. Scale bars, 500 nm.

Figure 2. Fundamental structural units of the nucleoid. A closer observation of the nucleoid in the log phase revealed two different fibers with 40 nm (**A**, arrowheads) and 80 nm (A and **B**, arrows) widths. The solid lines represent the sites of section analysis that are depicted in the upper right corner of the image. The horizontal dotted lines on section analysis images indicate the half-maximum height. The histogram of the fiber width, together with a Gaussian-fitting curve, is depicted in (**C**) (bin size, 10 nm). The 80 nm fiber forms the loop structure (arrows, inside diameter 149.53 ± 13.06 nm, mean ± SD) in a partially lysed nucleoid in the log phase (B). Scale bars, 500 nm.

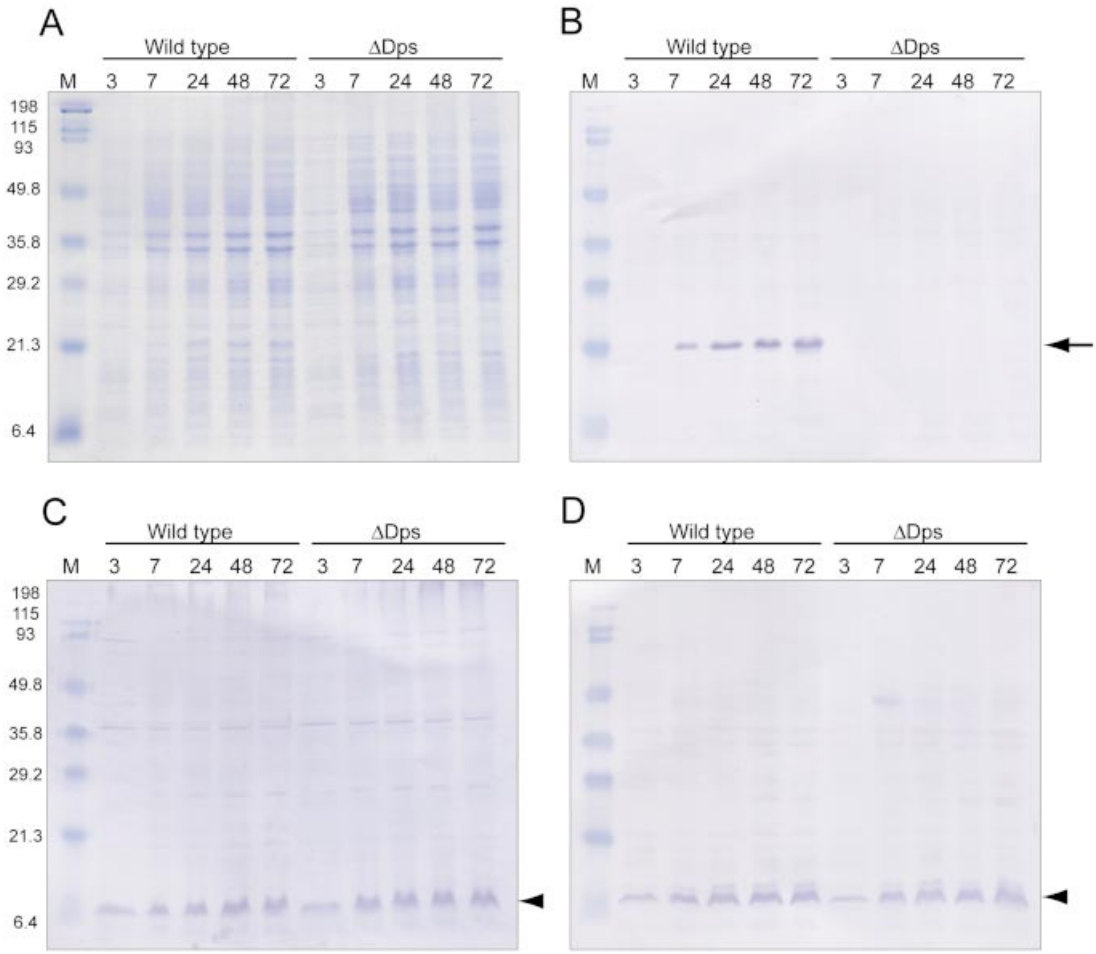

Figure 4. Western blot analysis of wild-type and ΔDps mutant cells. The protein compositions of the wild-type cells (lanes 1–5) and Dps-deficient cells (lanes 6–10) in each growth phase were analyzed by SDS–PAGE followed by Coomassie brilliant blue staining (**A**) or immunoblotting with polyclonal antibodies against Dps (**B**), HU (**C**) and IHF (**D**). Note that only Dps expression was abolished (arrow), and HU and IHF expression was not changed (arrowhead). It was demonstrated previously that HU (~9.5 kDa) and IHF (~11.4 kDa) migrate slightly faster than their expected molecular weights (46). The expression of H-NS, FIS and StpA was not affected (data not shown). Cells were grown in LB medium and harvested after 3, 7, 24, 48 or 72 h incubation. An equal amount of cell lysates was loaded in each well.

coral reef structure in the early stationary phase and still released the 80 nm fiber and the loop structures. In the late stationary phase, the nucleoid was still easy to lyse to expose the 40 and 80 nm fiber and loop structures (Fig. 5C), and was never transformed into the tightly packed state as seen in the wild-type nucleoid. This result proposes a critical role for the Dps protein in the higher order packing of the 80 nm fiber towards the stationary phase. Our preliminary analyses with *Clostridium* (which lacks the *dps* gene) showed that the nucleoid did not tightly compact in the stationary phase (data not shown).

To further examine the possible role of Dps, the Δ*dps* strain was subjected to a complementation test. The plasmid carrying the coding sequence of the *dps* gene under the control of the pT5/*lac* promoter was introduced into the W3110(Δ*dps*) strain. The addition of IPTG (5 mM) induced the expression of Dps within 1 h (Fig. 6A). The amount of protein reached the maximum level within 1 h and stayed almost constant for >18 h. When observed by AFM, the nucleoid in the stationary phase cells without induction (Fig. 6B) showed a similar structure to that without the plasmid (Fig. 5C), demonstrating that the existence of the plasmid in the absence of IPTG had no apparent effect on the structure of the nucleoid. When Dps expression was induced by IPTG in the stationary phase, the nucleoid started to become tightly packed after 20 min, and became completely packed after 40 min of induction (Fig. 6C), indicating that exogeneous Dps can swiftly induce nucleoid compaction in the stationary phase. On the other hand, when Dps was expressed in the log phase, the nucleoid was not condensed until the cells entered the stationary phase (Fig. 6D) (see Discussion).

DISCUSSION

In this study, we developed an 'on-substrate lysis procedure' suitable for specimen preparation for AFM. This on-substrate procedure has a good advantage over the biochemical methods

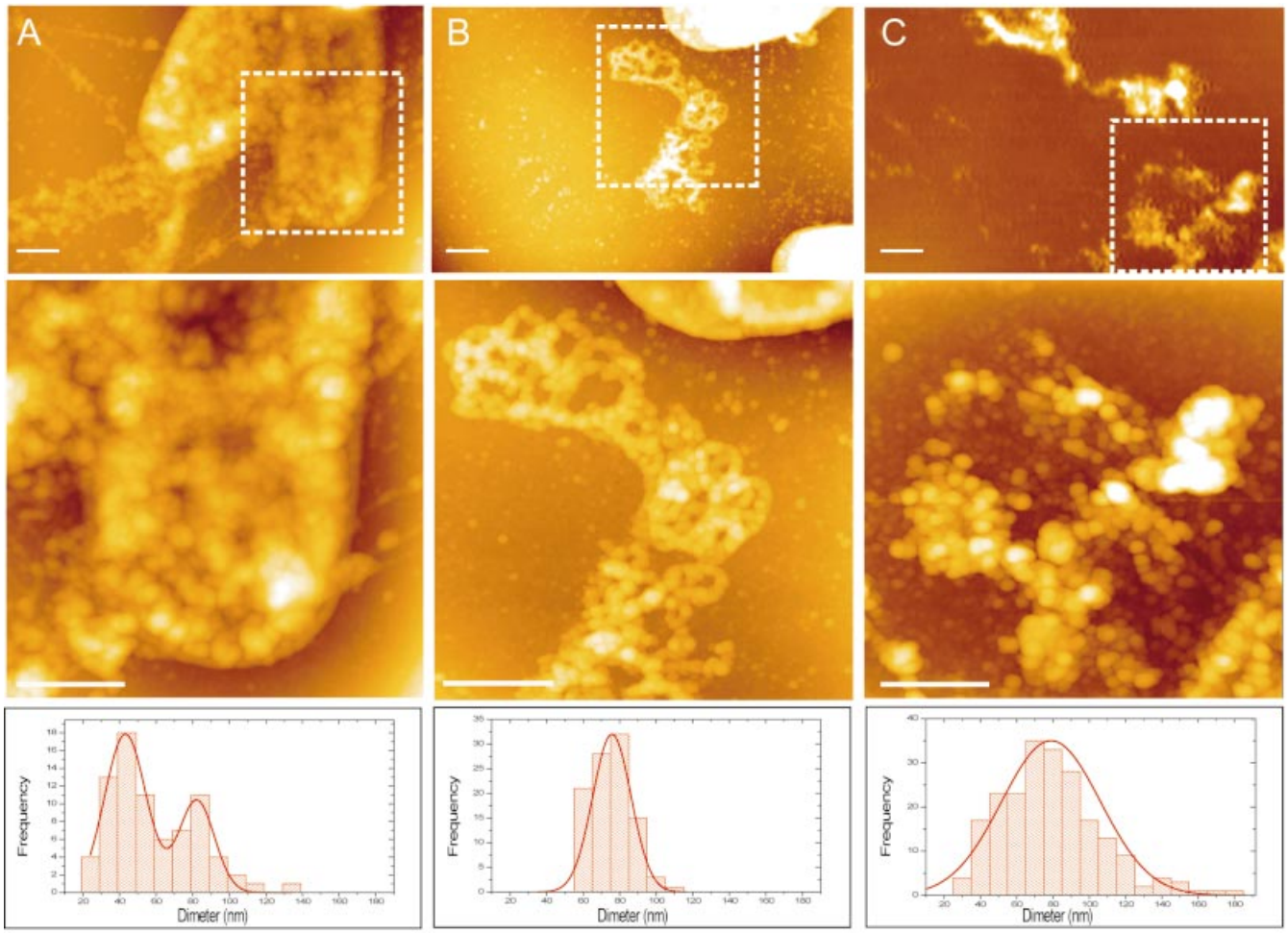

Figure 5. Dps induces a tight compaction of nucleoid in the stationary phase. Dps-deficient mutant strain W3110 was cultured and harvested in the log (**A**), early stationary (**B**) or late stationary (**C**) phases. The areas within dotted squares were rescanned and are shown in the middle panels. The cells were subjected to the same lysis treatment as in Figure 1 and observed by AFM. The loop structure (inside diameter 128.50 ± 17.78 nm, mean ± SD) was observed in all growing phases. The statistical analyses of the fiber width are summarized in the bottom panels (bin size, 10 nm). Scale bars, 500 nm.

involving purification steps on a sucrose density gradient, because it allows structural observations of individual nucleoids with minimum mechanical disturbance. Using this procedure, we demonstrated that the nucleoid of growing *E.coli* consisted of several hierarchical higher order structures; the 40 and 80 nm fibers and the loop structures.

The overall packaging status of the nucleoid changed greatly during cell growth, as evidenced by fluorescence microscopy and AFM (Fig. 1). Namely, the mild detergent treatment released the 40 and 80 nm fibers from the log phase nucleoid, but not from the stationary phase ones. The different sensitivities to the detergent should reflect the differences in nucleoid packing; the log phase nucleoid is more loosely packed than the stationary phase nucleoid. This growth-dependent difference in nucleoid packing is thought to be tightly coupled to the transcriptional and replicational activities of the genome.

The 40 and 80 nm fibers play a central role in nucleoid packing

The close observation of the log phase nucleoid revealed two types of thin fiber with diameters of ~80 and ~40 nm (Fig. 2A). Since the 80 nm fiber has a repetitive unit with 40 nm pitches, a helical self-assembly of the 40 nm fiber is thought to produce the 80 nm fiber. It is important to note that the 40 nm fiber frequently appeared in rapidly growing cells and that fibers thinner than 40 nm could not be released in any of the growth phases. Therefore, it is reasonable to assume that the 40 nm fiber could be a basic genome structure and more functional (active in transcription) than the 80 nm fiber. Indeed, the 80 nm fibers can still be seen inside the cells from the lag to the early stationary phases. Thus, the 80 nm fiber might be related to transcriptional inactivation.

The log phase cells which were partially lysed showed the 80 nm fiber forming a loop structure with an inside diameter of ~150 nm (Fig. 2B), indicating that a loop structure is a one-step higher order structure of the 80 nm fiber. Based on these observations, a hierarchical model of the nucleoid packing can be deduced (Fig. 7), in which the 40 nm fiber forms the 80 nm fiber by a helical self-assembly, and the 80 nm fiber forms the loop. The 40 nm fiber might be a structure corresponding to the 30 nm fiber in eukaryotic chromosome and is probably composed of histone-like proteins and other nucleoid-related proteins. The 'coral reef structure' in the early stationary phase

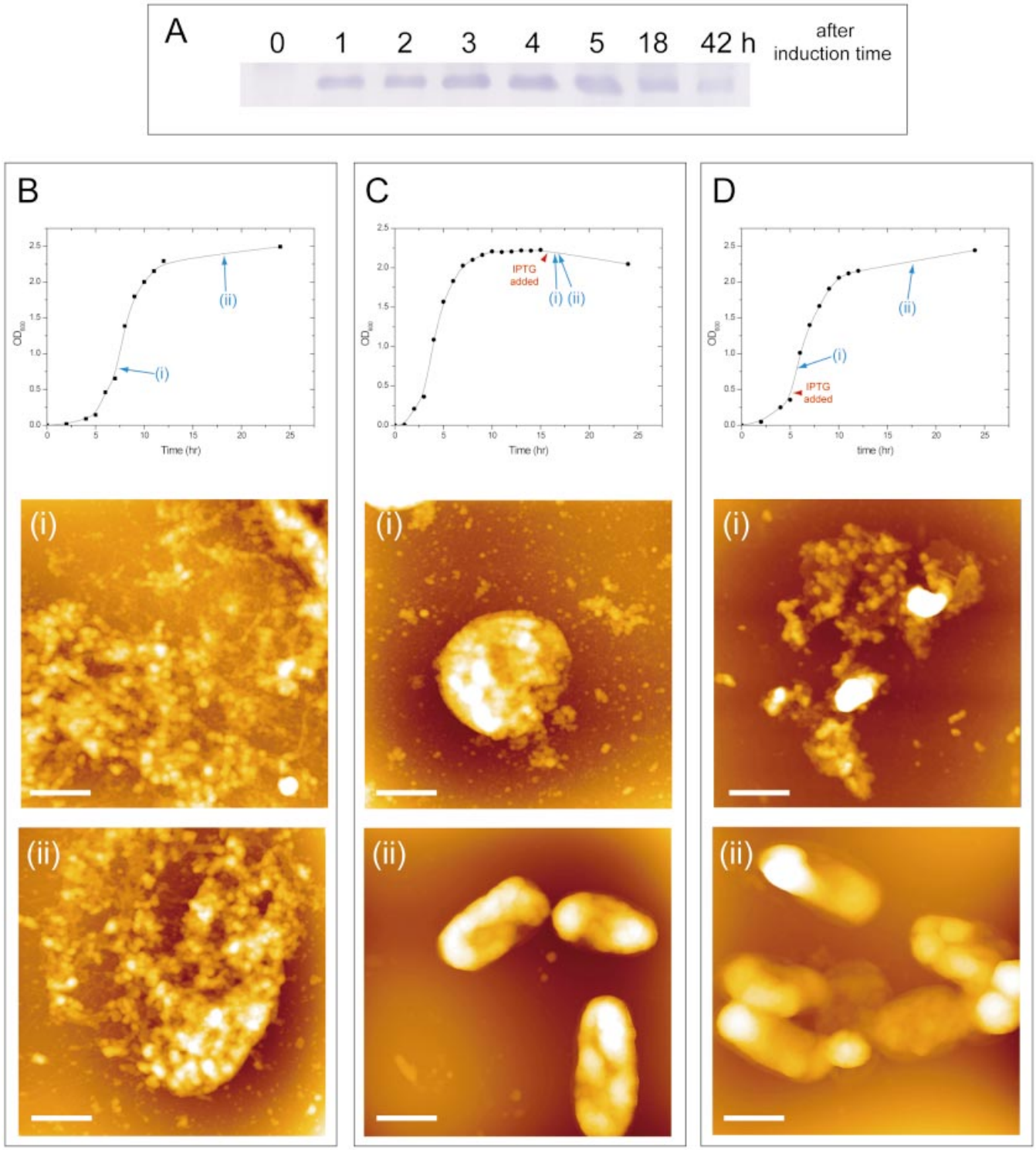

Figure 6. Complementation analysis of the Δ*dps* nucleoid structures. W3110 (Δ*dps*) cells carrying the plasmid pHM44 (Materials and Methods) were grown in LB medium and the expression of Dps protein was induced by IPTG (5 mM). (**A**) Immunoblot analysis of Dps protein. IPTG was added at OD = 0.2 (in the log phase) and the cells were collected at the indicated time after the induction and subjected to immunoblot analysis using anti-Dps antibody. (B–D) AFM analysis of the nucleoid structure. The expression of the Dps protein was not induced (**B**) or was induced with IPTG in the stationary phase (**C**) or in the log phase (**D**). The addition of IPTG did not affect cell growth (top panels). The cells were collected at the indicated time (i and ii) and subjected to observation by AFM (bottom panels). Scale bars, 1 µm.

might reflect a specific structure previously observed in stationary phase cells (33). It can be speculated that in this structure, the 80 nm fiber is further folded up in a superhelical manner to form a globular surface topology. However, understanding of the detailed packing mechanism requires further investigations.

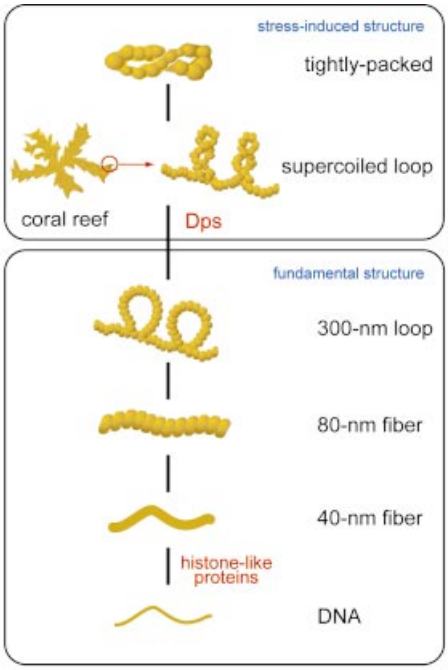

Figure 7. A model of nucleoid architecture. The DNA and histone-like proteins (HU, IHF, H-NS, etc.) form a nucleosome-like structure, which is further folded into a 40 nm fiber. The 40 nm fiber is supersolenoided into an 80 nm fiber with other nucleoid-related proteins. The 80 nm fiber forms a loop structure. These structures are thought to be fundamental structures of the nucleoid. The nucleoid becomes tightly packed and forms a coral reef structure of supercoiled 80 nm loops in the early stationary phase, and finally the tightly packed state in the late stationary phase. The formation of the coral reef structure is mainly mediated via a stress-induced protein, Dps.

Dps causes a tight compaction of the nucleoid in response to starvation

When the cells reached the stationary phase, the nucleoid structure was drastically changed into a tightly compacted configuration (Fig. 1). Since the Dps mutant cells did not show such a tight compaction of nucleoids in the stationary phase (Fig. 5), and since, throughout their cell growth, they still retained the 80 nm fiber and the loop structure, but not the coral reef structure (Fig. 5), this tight compaction of the nucleoid is mediated by Dps. The complementation experiments showed that the highly compacted structures were induced in the Δ*dps* strain in the stationary phase when the Dps protein was expressed, which supports the critical role of Dps in nucleoid compaction (Fig. 6C). However, Dps expressed in the log phase did not immediately induce the nucleoid compaction, although the intracellular amount of Dps reached the maximum level (Fig. 6D). These results suggest that an as yet unidentified mechanism should cooperate with Dps for the compaction. It is also possible that some proteins in log phase might prohibit the Dps protein from binding to DNA, because Dps itself can directly bind to DNA *in vitro* (34,35). These issues need to be resolved in the future.

The Dps protein was first identified as a stress-induced protein (26). It is a small peptide of mol. wt 19 kDa and is known to form a dodecameric complex (36). It binds to DNA without sequence specificity (26). The amount of Dps in the log phase is very low (~7000 molecules/cell) compared with other nucleoid-related proteins (~60 000 molecules/cell for Fis, Hfq and HU) (37). However, in the stationary phase, Dps becomes the most abundant protein (180 000 molecules/cell). It has previously been reported that over-expressed Dps proteins induce an intracellular crystalline structure *in vivo* (34,35). A similar phenomenon was also observed *in vitro*; purified Dps proteins co-crystallized with DNA (34,35). The highly compacted nucleoid observed in the late stationary phase had characteristics shared with such a bio-crystal that was tightly compacted and completely resistant to the detergent treatment. Bacterial cells might protect their own nucleoid from environmental stresses by forming this kind of tightly compacted configuration that is resistant to chemical and enzymatic reactions. Indeed, the Dps mutant cells are very sensitive to environmental stress (26,38). The formation of the coral reef structure might be the first step towards this tight compaction, and the Dps protein plays a critical role in achieving such a higher order structure.

Escherichia coli contains many DNA-binding proteins, only some of which are involved in the nucleoid configuration as the core nucleoid proteins. In log phase cells, several species of proteins, including Fis, Hfq, HU, StpA and H-NS, occupy the major surface of genomic DNA, while Dps and IHF are the major nucleoid proteins in stationary phase cells (37). These structural proteins influence the transcriptional level of sets of genes depending on their DNA-binding sites relative to the RNA polymerase-binding sites (39–41). Among these core nucleoid proteins, Dps and HU/IHF appear particularly important for the formation of a specific nucleoid configuration because these proteins exist in a wide range of members of the bacterial kingdom (Table 1). Detailed comparative examination of the nucleoid architecture lacking Fis, H-NS/StpA or Dps seems to be important for future investigations.

The 80 nm fiber: a fundamental structure in chromosome packing

In the human mitotic chromosome, 70–80 nm granular structures were identified by electron microscopy (42) and AFM (43). AFM also detected similar granules (~75 nm in diameter) in the interphase chromosomes of HeLa cells (44). In the mitotic chromosome of *Drosophila melanogaster*, fibrous structures of ~40 and ~80 nm widths were observed by electron microcopy (45). In this study, by using AFM, we demonstrated that the *E.coli* nucleoid consists of several hierarchical higher order structures; the 40 and 80 nm fibers and the loop structures. These lines of evidence suggest that the 30–40 nm thin fiber and the 70–80 nm granular fiber are fundamental structural units of the chromosome/nucleoid in eukaryotes and prokaryotes. Further detailed investigations of the chromosome folding mechanism in both eukaryotes and prokaryotes are required to test this possibility.

ACKNOWLEDGEMENTS

The plasmid pHM44 was a kind gift from Dr M. Kitagawa, Nara Institute of Technology, Japan. This work was supported by a CREST research project of the Japan Science and Technology Corporation, Special Co-ordination Funds and a COE Research Grant from the Ministry of Education, Culture,

Table 1. Distribution of *E.coli* nucleoid proteins in bacterial species

			Hu/ IHF	H-NS/ StpA	Dps	Fis	CbpA	DnaA	CbpB	Hfq	IciA/ LysR	Lrp/ AsnC
Proteobacteria	γ	*Escherichia coli* K-12 MG1655	+	+	+	+	+	+	+	+	+	+
		Escherichia coli K-12 W3110	+	+	+	+	+	+	+	+	+	+
		Escherichia coli O157 EDL933	+	+	+	+	+	+	+	+	+	+
		Escherichia coli O157 Sakai	+	+	+	+	+	+	+	+	+	+
		Escherichia coli CFT073	+	+	+	+	+	+	+	+	+	+
		Salmonella typhi CT18	+	+	+	+	+	+	+	+	+	+
		Salmonella typhimurium	+	+	+	+	+	+	+	+	+	+
		Yersinia pestis CO92	+	+	+	+	–	+	+	+	+	+
		Yersinia pestis KIM	+	+	+	+	–	+	+	+	+	+
		Shigella flexneri 301 (serotype 2a)	+	+	+	+	+	+	+	+	+	+
		Buchnera sp. APS (*Acyrthosiphon pisum*)	+	+	–	+	–	+	–	–	–	–
		Buchnera aphidicola (*Schizaphis graminum*)	+	–	–	+	–	+	–	–	+	–
		Buchnera aphidicola (*Baizongia pistaciae*)	+	–	–	–	–	+	–	–	–	–
		Wigglesworthia brevipalpis	+	+	–	–	–	–	–	+	–	–
		Haemophilus influenzae	+	+	+	+	–	+	–	+	+	+
		Pasteurella multocida	+	+	+	+	–	+	–	+	+	+
		Xylella fastidiosa 9a5c	+	+	+	+	+	+	–	+	+	–
		Xylella fastidiosa Temecula1	+	+	+	+	+	+	–	+	+	–
		Xanthomonas campestris	+	+	+	+	+	+	–	+	+	+
		Xanthomonas axonopodis	+	+	+	+	+	+	–	+	+	+
		Vibrio cholerae	+	+	+	+	–	+	–	+	+	+
		Vibrio vulnificus	+	+	+	+	–	+	+	+	+	+
		Vibrio parahaemolyticus	+	+	+	+	–	+	–	+	+	+
		Pseudomonas aeruginosa	+	+	+	+	–	+	+	+	+	+
		Shewanella oneidensis	+	+	+	+	–	+	–	+	+	+
		Coxiella burnetii	+	–	–	+	+	+	–	–	–	–
	β	*Neisseria meningitidis* MC58 (serogroup B)	+	–	–	+	–	+	–	+	+	+
		Neisseria meningitidis Z2491 (serogroup A)	+	–	–	+	–	+	–	+	+	+
		Ralstonia solanacearum	+	+	+	+	–	+	+	+	+	+
	δ/ε	*Helicobacter pylori* 26695	+	–	+	–	+	+	–	–	–	–
		Helicobacter pylori J99	+	–	+	–	+	+	+	–	–	–
		Campylobacter jejuni	+	–	+	–	+	+	–	–	–	–
	α	*Rickettsia prowazekii*	+	–	+	–	–	+	–	–	–	–
		Rickettsia conorii	+	–	–	–	–	+	–	–	–	–
		Mesorhizobium loti	+	–	–	–	–	+	+	+	+	+
		Sinorhizobium meliloti	+	–	–	–	+	+	+	+	+	+
		Agrobacterium tumefaciens C58 (UWash/Dupont)	+	–	+	–	–	+	+	+	+	+
		Agrobacterium tumefaciens C58 (Cereon)	+	–	+	–	–	+	+	+	+	+
		Brucella melitensis	+	–	+	–	–	+	–	+	+	+
		Brucella suis	+	–	+	–	–	+	–	+	+	+
		Bradyrhizobium japonicum	+	–	+	–	+	+	+	+	+	+
		Caulobacter crescentus	+	–	+	–	–	+	+	+	+	+
Firmicutes	Bacillales	*Bacillus subtilis*	+	–	+	–	–	+	+	+	+	+
		Bacillus halodurans	+	–	+	–	–	+	+	+	+	+
		Bacillus anthracis	+	–	+	–	–	+	+	+	+	+
		Bacillus cereus	+	–	+	–	–	+	+	+	+	+
		Oceanobacillus iheyensis	+	–	+	–	–	+	+	+	+	+
		Staphylococcus aureus N315 (MRSA)	+	–	+	–	–	+	–	+	+	–
		Staphylococcus aureus Mu50 (VRSA)	+	–	+	–	–	+	–	+	+	–
		Staphylococcus aureus MW2	+	–	+	–	–	+	–	+	+	–
		Staphylococcus epidermidis	+	–	+	–	–	+	–	+	+	–
		Listeria monocytogenes	+	–	+	–	–	+	–	+	+	–
		Listeria innocua	+	–	+	–	–	+	+	+	+	–
	Lactobacillales	*Lactococcus lactis*	+	–	+	–	–	+	–	–	+	–
		Streptococcus pyogenes SF370 (serotype M1)	+	–	+	–	–	+	–	–	+	–
		Streptococcus pyogenes MGAS8232 (serotype M18)	+	–	+	–	–	+	–	–	+	–
		Streptococcus pyogenes MGAS315 (serotype M3)	+	–	+	–	–	+	–	–	+	–

Table 1. *Continued*

			Hu/ IHF	H-NS/ StpA	Dps	Fis	CbpA	DnaA	CbpB	Hfq	IciA/ LysR	Lrp/ AsnC
		Streptococcus pneumoniae TIGR4	+	–	+	–	–	+	–	–	+	–
		Streptococcus pneumoniae R6	+	–	+	–	–	+	–	–	+	–
		Streptococcus mutans	+	–	+	–	–	+	–	–	+	–
		Lactobacillus plantarum	+	–	+	–	–	+	–	–	+	+
		Enterococcus faecalis	+	–	+	–	–	+	–	–	+	–
	Clostridia	*Clostridium acetobutylicum*	+	–	–	–	–	+	+	+	+	+
		Clostridium perfringens	+	–	–	–	–	+	–	+	+	+
		Clostridium tetani	+	–	–	–	–	+	+	+	+	+
		Thermoanaerobacter tengcongensis	+	–	–	–	–	+	–	+	+	+
	Mollicutes	*Mycoplasma genitalium*	–	–	–	–	–	+	–	–	–	–
		Mycoplasma pneumoniae	–	–	–	–	–	+	–	–	–	–
		Mycoplasma pulmonis	+	–	–	–	–	+	–	–	–	–
		Mycoplasma penetrans	+	–	–	–	–	+	–	–	–	–
		Ureaplasma urealyticum	+	–	–	–	–	+	–	–	–	–
Actinobacteria		*Mycobacterium tuberculosis* H37Rv (lab strain)	+	–	–	–	–	+	–	–	+	+
		Mycobacterium tuberculosis CDC1551	+	–	–	–	–	+	–	–	+	+
		Mycobacterium leprae	+	–	–	–	–	+	–	–	+	+
		Corynebacterium glutamicum	–	–	+	–	–	+	–	–	+	+
		Corynebacterium efficiens	–	–	+	–	–	+	–	–	+	+
		Streptomyces coelicolor	+	–	+	–	–	+	+	–	+	+
		Bifidobacterium longum	+	–	+	–	–	+	–	–	+	+
		Tropheryma whipplei Twist	+	–	+	–	+	+	–	–	–	–
		Tropheryma whipplei TW08/27	+	–	+	–	+	+	–	–	–	–
Fusobacteria		*Fusobacterium nucleatum*	+	–	+	–	–	–	–	–	+	–
Chlamydia		*Chlamydia trachomatis*	+	–	–	–	–	+	–	–	–	–
		Chlamydia muridarum	+	–	–	–	–	+	–	–	–	–
		Chlamydophila pneumoniae CWL029	+	–	–	–	–	+	–	–	–	–
		Chlamydophila pneumoniae AR39	+	–	–	–	–	+	–	–	–	–
		Chlamydophila pneumoniae J138	+	–	–	–	–	+	–	–	–	–
		Chlamydophila caviae	+	–	–	–	–	+	–	–	–	–
Spirochete		*Borrelia burgdorferi*	+	–	+	–	+	+	–	–	–	–
		Treponema pallidum	+	–	+	–	–	+	–	–	–	–
		Leptospira interrogans	+	–	+	–	–	+	–	+	–	–
Cyanobacteria		*Synechocystis* sp. PCC6803	+	–	+	–	+	+	–	–	+	–
		Thermosynechococcus elongatus	+	–	+	–	–	+	–	–	+	–
		Anabaena sp. PCC7120 (*Nostoc* sp. PCC7120)	+	–	+	–	+	+	–	–	+	–
Green sulfur bacteria		*Chlorobium tepidum*	+	–	–	–	–	+	–	–	–	+
Radioresistant bacteria		*Deinococcus radiodurans*	+	–	+	–	–	+	–	–	+	+
Hyperthermophilic bacteria		*Aquifex aeolicus*	+	–	–	–	–	+	–	+	–	–
		Thermotoga maritima	+	–	–	–	–	+	–	+	–	–

The presence (+) and absence (–) of orthologs [for CbpA, DnaA, CbpB, Dps, HU/IHF (paralogs), Hfq, Fis, H-NS/StpA (paralogs)] or closely related homologs (for IciA/LysR, Lrp/AsnC) in various bacterial species was determined by homolog search (SSDB and the FASTA) in the KEGG databases. It should be noted that H-NS, HU, IHF, StpA and Dps were distributed among many species, whereas CbpA, CbpB, Fis and IciA were detected only in the restricted ones.

Sports, Science and Technology of Japan. We also thank the Sasakawa Scientific Research Grant and the Sumitomo Foundation for their support. S.H.Y was a recipient of a pre-doctoral fellowship from the Japan Society for the Promotion of Science.

REFERENCES

1. Kornberg,R.D. and Lorch,Y. (1999) Chromatin-modifying and -remodeling complexes. *Curr. Opin. Genet. Dev.*, **9**, 148–151.
2. Yoshimura,S.H., Ohniwa,R.L., Sato,M.H., Matsunaga,F., Kobayashi,G., Uga,H., Wada,C. and Takeyasu,K. (2000) DNA phase transition promoted by replication initiator. *Biochemistry*, **39**, 9139–9145.
3. Gross,D.S. and Garrard,W.T. (1988) Nuclease hypersensitive sites in chromatin. *Annu. Rev. Biochem.*, **57**, 159–197.
4. Simpson,R.T. (1986) Nucleosome positioning *in vivo* and *in vitro*. *Bioessays*, **4**, 172–176.
5. Svaren,J. and Chalkley,R. (1990) The structure and assembly of active chromatin. *Trends Genet.*, **6**, 52–56.
6. Travers,A.A. and Klug,A. (1987) The bending of DNA in nucleosomes and its wider implications. *Philos. Trans. R. Soc. Lond. B Biol. Sci.*, **317**, 537–561.
7. Wolffe,A.P. (1998) Packaging principle: how DNA methylation and histone acetylation control the transcriptional activity of chromatin. *J. Exp. Zool.*, **282**, 239–244.
8. Zhang,L. and Gralla,J.D. (1990) *In situ* nucleoprotein structure involving origin-proximal SV40 DNA control elements. *Nucleic Acids Res.*, **18**, 1797–1803.

9. Kornberg,R.D. and Lorch,Y. (1999) Twenty-five years of the nucleosome, fundamental particle of the eukaryote chromosome. *Cell*, **98**, 285–294.
10. Zlatanova,J., Leuba,S.H. and van Holde,K. (1998) Chromatin fiber structure: morphology, molecular determinants, structural transitions. *Biophys. J.*, **74**, 2554–2566.
11. Sato,M.H., Ura,K., Hohmura,K.I., Tokumasu,F., Yoshimura,S.H., Hanaoka,F. and Takeyasu,K. (1999) Atomic force microscopy sees nucleosome positioning and histone H1-induced compaction in reconstituted chromatin. *FEBS Lett.*, **452**, 267–271.
12. Karymov,M.A., Tomschik,M., Leuba,S.H., Caiafa,P. and Zlatanova,J. (2001) DNA methylation-dependent chromatin fiber compaction *in vivo* and *in vitro*: requirement for linker histone. *FASEB J.*, **15**, 2631–2641.
13. Hohmura,K.I., Itokazu,Y., Yoshimura,S.H., Mizuguchi,G., Masamura,Y.S., Takeyasu,K., Shiomi,Y., Tsurimoto,T., Nishijima,H., Akita,S. *et al.* (2000) Atomic force microscopy with carbon nanotube probe resolves the subunit organization of protein complexes. *J. Electron Microsc.*, **49**, 415–421.
14. Bloom,K.S. and Carbon,J. (1982) Yeast centromere DNA is in a unique and highly ordered structure in chromosomes and small circular minichromosomes. *Cell*, **29**, 305–317.
15. Kornberg,R.D. (1974) Chromatin structure: a repeating unit of histones and DNA. *Science*, **184**, 868–871.
16. Murray,A.W. and Szostak,J.W. (1983) Construction of artificial chromosomes in yeast. *Nature*, **305**, 189–193.
17. Thoma,F., Koller,T. and Klug,A. (1979) Involvement of histone H1 in the organization of the nucleosome and of the salt-dependent superstructures of chromatin. *J. Cell Biol.*, **83**, 403–427.
18. Narlikar,G.J., Fan,H.Y. and Kingston,R.E. (2002) Cooperation between complexes that regulate chromatin structure and transcription. *Cell*, **108**, 475–487.
19. Bechtloff,D., Grunenfelder,B., Akerlund,T. and Nordstrom,K. (1999) Analysis of protein synthesis rates after initiation of chromosome replication in *Escherichia coli*. *J. Bacteriol.*, **181**, 6292–6299.
20. Rouviere-Yaniv,J., Yaniv,M. and Germond,J.E. (1979) *E.coli* DNA binding protein HU forms nucleosomelike structure with circular double-stranded DNA. *Cell*, **17**, 265–274.
21. Tanaka,I., Appelt,K., Dijk,J., White,S.W. and Wilson,K.S. (1984) 3-Å resolution structure of a protein with histone-like properties in prokaryotes. *Nature*, **310**, 376–381.
22. Dorman,C.J., Hinton,J.C. and Free,A. (1999) Domain organization and oligomerization among H-NS-like nucleoid-associated proteins in bacteria. *Trends Microbiol.*, **7**, 124–128.
23. McLeod,S.M. and Johnson,R.C. (2001) Control of transcription by nucleoid proteins. *Curr. Opin. Microbiol.*, **4**, 152–159.
24. Williams,R.M. and Rimsky,S. (1997) Molecular aspects of the *E.coli* nucleoid protein, H-NS: a central controller of gene regulatory networks. *FEMS Microbiol. Lett.*, **156**, 175–185.
25. Drlica,K. and Rouviere-Yaniv,J. (1987) Histonelike proteins of bacteria. *Microbiol. Rev.*, **51**, 301–319.
26. Almiron,M., Link,A.J., Furlong,D. and Kolter,R. (1992) A novel DNA-binding protein with regulatory and protective roles in starved *Escherichia coli*. *Genes Dev.*, **6**, 2646–2654.
27. Schneider,S.W., Larmer,J., Henderson,R.M. and Oberleithner,H. (1998) Molecular weights of individual proteins correlate with molecular volumes measured by atomic force microscopy. *Pflugers Arch.*, **435**, 362–367.
28. Mori,H., Isono,K., Horiuchi,T. and Miki,T. (2000) Functional genomics of *Escherichia coli* in Japan. *Res. Microbiol.*, **151**, 121–128.
29. Kanehisa,M., Goto,S., Kawashima,S. and Nakaya,A. (2002) The KEGG databases at GenomeNet. *Nucleic Acids Res.*, **30**, 42–46.
30. Cunha,S., Odijk,T., Suleymanoglu,E. and Woldringh,C.L. (2001) Isolation of the *Escherichia coli* nucleoid. *Biochimie*, **83**, 149–154.
31. Hinnebusch,B.J. and Bendich,A.J. (1997) The bacterial nucleoid visualized by fluorescence microscopy of cells lysed within agarose: comparison of *Escherichia coli* and spirochetes of the genus *Borrelia*. *J. Bacteriol.*, **179**, 2228–2237.
32. Thony,B., Hwang,D.S., Fradkin,L. and Kornberg,A. (1991) *iciA*, an *Escherichia coli* gene encoding a specific inhibitor of chromosomal initiation of replication *in vitro*. *Proc. Natl Acad. Sci. USA*, **88**, 4066–4070.
33. Bohrmann,B., Villiger,W., Johansen,R. and Kellenberger,E. (1991) Coralline shape of the bacterial nucleoid after cryofixation. *J. Bacteriol.*, **173**, 3149–3158.
34. Wolf,S.G., Frenkiel,D., Arad,T., Finkel,S.E., Kolter,R. and Minsky,A. (1999) DNA protection by stress-induced biocrystallization. *Nature*, **400**, 83–85.
35. Frenkiel-Krispin,D., Levin-Zaidman,S., Shimoni,E., Wolf,S.G., Wachtel,E.J., Arad,T., Finkel,S.E., Kolter,R. and Minsky,A. (2001) Regulated phase transitions of bacterial chromatin: a non-enzymatic pathway for generic DNA protection. *EMBO J.*, **20**, 1184–1191.
36. Grant,R.A., Filman,D.J., Finkel,S.E., Kolter,R. and Hogle,J.M. (1998) The crystal structure of Dps, a ferritin homolog that binds and protects DNA. *Nature Struct. Biol.*, **5**, 294–303.
37. Talukder,A.A., Iwata,A., Nishimura,A., Ueda,S. and Ishihama,A. (1999) Growth phase-dependent variation in protein composition of the *Escherichia coli* nucleoid. *J. Bacteriol.*, **181**, 6361–6370.
38. Martinez,A. and Kolter,R. (1997) Protection of DNA during oxidative stress by the nonspecific DNA-binding protein Dps. *J. Bacteriol.*, **179**, 5188–5194.
39. Ishihama,A. (1999) Modulation of the nucleoid, the transcription apparatus and the translation machinery in bacteria for stationary phase survival. *Genes Cells*, **4**, 135–143.
40. Goosen,N. and van de Putte,P. (1995) The regulation of transcription initiation by integration host factor. *Mol. Microbiol.*, **16**, 1–7.
41. Finkel,S.E. and Johnson,R.C. (1992) The Fis protein: it's not just for DNA inversion anymore. *Mol. Microbiol.*, **6**, 3257–3265.
42. Adolph,K.W., Kreisman,L.R. and Kuehn,R.L. (1986) Assembly of chromatin fibers into metaphase chromosomes analyzed by transmission electron microscopy and scanning electron microscopy. *Biophys. J.*, **49**, 221–231.
43. Tamayo,J. and Miles,M. (2000) Human chromosome structure studied by scanning force microscopy after an enzymatic digestion of the covering cell material. *Ultramicroscopy*, **82**, 245–251.
44. Yoshimura,S.H., Kim,J. and Takeyasu,K. (2003) On-substrate lysis treatment combined with scanning probe microscopy revealed chromosome structures in eukaryotes and prokaryotes. *J. Electron Microsc.*, **52**, 415–423.
45. Belmont,A.S., Sedat,J.W. and Agard,D.A. (1987) A three-dimensional approach to mitotic chromosome structure: evidence for a complex hierarchical organization. *J. Cell Biol.*, **105**, 77–92.
46. Azam,T.A. and Ishihama,A. (1999) Twelve species of the nucleoid-associated protein from *Escherichia coli*. Sequence recognition specificity and DNA binding affinity. *J. Biol. Chem.*, **274**, 33105–33113.